Bone-Targeting of Quinolones Conjugated with an Acidic Oligopeptide

Research paper

Bone-targeting of quinolones conjugated with an acidic oligopeptide

Tatsuo Takahashi[a], Koichi Yokogawa[b], Naoki Sakura[c], Masaaki Nomura[a], Shinjiro Kobayashi[a, d], Ken-ichi Miyamoto[b, *]

[a]Department of Clinical Pharmacology and [c]Department of Biosynthetic Chemistry; Faculty of Pharmaceutical Sciences

[d]Organization for Frontier Research in Preventive Pharmaceutical Sciences, Hokuriku University, Kanazawa 920-1181, Japan

[b]Department of Medicinal Informatics; Graduate School of Medical Science, Kanazawa University, Kanazawa 920-8641, Japan

* To whom correspondence should be addressed: Department of Medicinal Informatics, Graduate School of Medical Science, Kanazawa University, 13-1 Takara-machi, Kanazawa 920-8641, Japan

Tel: +81-76-265-2045; Fax: +81-76-234-4280; E-mail: miyaken@pharmacy.m.kanazawa-u.ac.jp

Abstract

Purpose: Osteomyelitis is a progressive infectious process resulting in inflammatory destruction and necrosis of bone. The long-term administration of high-dosage antibiotics is required to treat osteomyelitis, owing to the limited distribution of antibiotics within bone. Therefore, targeted delivery of antibiotics to bone promises to improve therapeutic effectiveness. **Methods**: We synthesized quinolones such as levofloxacin and norfloxacin conjugated to an acidic oligopeptide, which works as a bone-targeting carrier after systemic administration. The therapeutic effectiveness of the conjugated quinolones in osteomyelitis was evaluated using a mouse model of osteomyelitis, created by inoculating *Staphylococcus aureus* into the tibia of mice. **Results**: With intravenous injection, the conjugated quinolones selectively distributed to bone, reaching concentrations up to 100-fold those of non-conjugated quinolones. Single intravenous injection of levofloxacin as well as conjugated levofloxacin exhibited antibiotic effects in the osteomyelitis mouse model; conversely, neither conjugated nor non-conjugated norfloxacin was effective. The antibiotic effect of conjugated levofloxacin persisted to at least 6 days after injection, whereas the effect of non-conjugated levofloxacin was temporary. **Conclusion**: The selective bone delivery of quinolones conjugated with an acidic oligopeptide may be effective in treating osteomyelitis, although the resulting concentration of antibiotic may be insufficient to completely kill *S. aureus*.

Introduction

　　Osteomyelitis is an inflammation of bone marrow and surrounding cortical bone that results in bone destruction and necrosis. Historically, osteomyelitis has been categorized as acute, subacute, or chronic based on the time of disease onset. Acute osteomyelitis develops within 2 weeks after disease onset; subacute osteomyelitis, within one to several months; and chronic osteomyelitis, after a few months. *Staphylococcus aureus* is commonly implicated in most cases of acute and chronic osteomyelitis and is responsible for up to 90% of acute hematogenous osteomyelitis in children. In adults, osteomyelitis most often results from the contiguous spread of microbes, usually involving multiple organisms (1-4). Acute hematogenous osteomyelitis is managed by careful evaluation of microbial etiology and susceptibility, and a 4- to 6-week course of appropriate antibiotic therapy (5). Chronic osteomyelitis is generally treated with surgical debridement and the administration of parental antibiotics such as β-lactams or aminoglycosides. Without adequate debridement, most antibiotic regimens fail, even with prolonged therapy. After the removal of necrotic tissue, the remaining bed of tissues must be considered to be contaminated with the responsible pathogens. Antibiotic treatment for at least 4 weeks is recommended (3, 6, 7). Moreover, the serum bactericidal titer, which is defined as the maximal dilution of serum able to kill the infecting organism *in vitro*, should be at least 1:2 for acute osteomyelitis treatment and at least 1:4 for chronic osteomyelitis treatment (8). The long-term administration of high-dosage antibiotics is required to treat osteomyelitis, owing to a lack of antibiotic penetration into bone tissue.

　　Various studies have suggested that the local application of antibiotics using antibiotic-impregnated bioimplants such as polymethylmethacrylate beads, hydroxyapatite bone cement, or biodegradable microspheres provide higher local antibiotic concentrations than those achievable with intravenous administration, with the additional advantage of avoiding toxicity associated with high levels of drug in the plasma (9-14). However, the bioimplant methodology appears to be useful only in chronic osteomyelitis, because surgical debridement is not necessary in acute osteomyelitis. Furthermore, the invasive procedure required for placing bioimplants may

result in secondary bone infections. Therefore, the development of non-invasive approaches, including oral antibiotics that target the bone, can enhance the clinical accessibility and convenience of antibiotic therapy for osteomyelitis patients.

Recently, a novel drug delivery system using acidic oligopeptides to target the bone was proposed. This unique approach is based on the physical properties of several non-collagenous bone proteins that have repetitive sequences of acidic amino acids (L-Asp or L-Glu) and bind to hydroxyapatite (15-17). Osteopontin and bone sialoprotein, two major non-collagenous proteins in bone, have L-Asp and L-Glu repetitive sequences, respectively, and rapidly bind to hydroxyapatite after secretion in osteoblastic cell culture (18-20). To determine the binding affinity of acidic oligopeptides to hydroxyapatite, homopeptides consisting of two to ten residues of acidic amino acids were conjugated with 9-fluorenylmethylchloroformate and the binding affinities were investigated *in vitro*. The results indicated that the dissociation constants of the acidic oligopeptides decreased with increasing numbers of acidic amino acid residues, and the maximal binding rates reached a plateau at six residues, which were independent of acidic amino acid specie (Asp or Glu) and optical isomeric form (L or D) (21). *In vivo*, fluorescein-labeled L-Asp hexapeptide accumulated specifically in bone at 24 h after systemic administration in mice and was not detected in other tissues. Surprisingly, fluorescein-labeled L-Asp hexapeptide was detectable in bone 14 days after administration (22).

Quinolones such as levofloxacin (LVFX) and norfloxacin (NFLX) have a broad spectrum of activity *in vitro*, including activity against the Gram negative organisms, *S. aureus* and *S. epidermidis*; therefore, increasing the quinolone concentration in bone should increase therapeutic effectiveness in patients with osteomyelitis (23-25). In the present study, we conjugated L-Asp hexapeptides to LVFX and NFLX, and evaluated their bone-targeting properties and therapeutic effectiveness in a mouse model of osteomyelitis.

Materials and Methods

Synthesis of L-Asp hexapeptide-conjugated levofloxacin

LVFX was esterified with glycolic acid before conjugation to L-Asp hexapeptide. Oxalyl chloride (2.76 mmol) was added to a cooled solution of LVFX (1.38 mmol) in dichloromethane (15 ml) including dimethylformamide (DMF; 0.1 ml), and the reaction mixture was stirred for 2 h at room temperature. Dichloromethane and unreacted oxalyl chloride were evaporated, and the samples were left until completely dry. The residue was dissolved in dichloromethane (10 ml), then dimethylaminopyridine (4.15 mmol) and benzyl glycolate (1.66 mmol) were added, and the solution was stirred overnight at 4°C. The resulting benzyl glycolyl ester of LVFX was purified by reverse-phase high performance liquid chromatography (RP-HPLC) with a YMC D-ODS-5 120A column (20 × 250 mm, YMC Co. Ltd., Kyoto, Japan) in 0.1% trifluoroacetic acid (TFA)-acetonitrile solvent at a flow rate of 8 ml/min and with monitoring at 210 nm. For the removal of benzyl by catalytic reduction, the benzyl glycolyl ester of LVFX was dissolved in methanol (10 ml) containing 0.5 ml of 50% acetic acid, and then a palladium suspension was added. The reaction mixture was stirred in a stream of hydrogen for 5 h at room temperature, followed by purification with RP-HPLC as described above. The resulting glycolyl ester of LVFX (LVFX-ga) was used in the conjugation reaction with L-Asp hexapeptide.

Starting with hydroxymethylphenoxymethyl resin (HMP resin or Wang resin) anchored with N^α-(9-fluorenylmethyloxycarbonyl)-L-aspartic acid β-tert-butyl ester [Fmoc-L-Asp(OBut)-OH], the Fmoc-[L-Asp(OBut)]$_6$-O-HMP-resin (0.30 mmol) was constructed using an Fmoc solid-phase method and a peptide synthesizer (ABI 433A; Applied Biosystems, CA, USA) and employing 2-(1H-benzotriazole-1-yl)-1,1,3,3-tetramethyluronium hexafluorophosphate (HBTU) as a coupling reagent. The peptide resin was treated with 20% piperidine in N-methylpyrolidone and was coupled with LVFX-ga (0.30 mmol) by N,N'-dicyclohexylcarbodiimide (DCC; 0.39 mmol) in a mixture of DMF (3 ml) and dichloromethane (15 ml) for 6 h. The resulting LVFX-ga-[Asp(OBut)]$_6$-O-HMP-resin was washed with DMF and dichloromethane-methanol (1:1) and was dried *in vacuo* prior to cleavage

and deprotection with 95% TFA (10 ml) at room temperature for 1.5 h. The resin was removed by filtration, and the filtrate was evaporated and lyophilized. The crude product was purified by RP-HPLC and lyophilized as described above. The synthesized LVFX-D_6 was subjected to fast atom bombardment-mass spectroscopy (FAB-MS) analysis (JMS-DX300 mass spectrometer, JEOL, Ltd., Tokyo, Japan).

Synthesis of L-Asp hexapeptide-conjugated norfloxacin

NFLX was amidated with glycolic acid, followed by esterification with succinic acid. To a mixture of NFLX (1.57 mmol), glycolic acid (1.57 mmol), and N-methylmorpholine (3.13 mmol) in DMF (25 ml) was added o-(7-azabenzotriazol-1-yl)-N,N,N',N'-tetramethyluronium hexafluorophosphate (1.57 mmol). The reaction mixture was stirred overnight at 4°C and then evaporated until dry. The residue was washed with 50% methanol, 5% acetic acid, and dH_2O. The resulting glycolyl-NFLX (NFLX-ga) was dried *in vacuo*. Succinic anhydride (3.18 mmol) was added to the mixture of NFLX-ga (1.06 mmol) and dimethylaminopyridine (3.18 mmol) in DMF (30 ml). The reaction mixture was stirred for 48 h at 4°C and then evaporated until dry. The residue was washed with 3% acetic acid and then with dH_2O, followed by drying *in vacuo*. The resulting NFLX-ga hemisuccinate (NFLX-ga-suc) was used for further conjugation with L-Asp hexapeptide.

NFLX-ga-suc (0.30 mmol) and H-[Asp(OBut)]$_6$-O-HMP-resin (0.30 mmol) were reacted in the presence of DCC (0.39 mmol) in the same manner as described above for the synthesis of L-Asp hexapeptide-conjugated LVFX. The product was obtained by treating the resin with 95% TFA, followed by purification with RP-HPLC and lyophilization. Synthesized NFLX-D_6 was subjected to FAB-MS analysis.

HPLC analysis

The concentrations of LVFX, LVFX-D_6, NFLX, NFLX-ga, and NFLX-D_6 were determined using an HPLC system (Shimadzu, Kyoto, Japan) equipped with a Shim-pack

CLC-ODS column (6 × 150 mm, Shimadzu). The mobile phase for LVFX, LVFX-D$_6$, NFLX, and NFLX-ga was 15% acetonitrile in 0.1% TFA, and that for NFLX-D$_6$ was 23% acetonitrile in 0.1% TFA. The flow rate was 1 ml/min. For fluorescence detection, the excitation and emission wavelengths were 296 nm and 500 nm, respectively, for LVFX and LVFX-D$_6$ and were 281 nm and 440 nm, respectively, for NFLX, NFLX-ga, and NFLX-D$_6$. The compounds were quantified by comparing the peak area ratio to standard curves generated from an internal standard (ciprofloxacin; CPFX).

Hydroxyapatite-binding assay

Hydroxyapatite beads (Bio-Rad Laboratories, CA, USA) were suspended in 50 mM Tris-HCl-buffered saline, pH 7.4, at a concentration of 100 μg/200 μl. LVFX, LVFX-D$_6$, NFLX, NFLX-ga, and NFLX-D$_6$ were respectively mixed with the hydroxyapatite suspension at final concentrations of 0.1, 0.3, 1.0, 3.0, 10.0, and 30 μM in a 400-μl final volume. The mixtures were agitated at 37°C for 1 h, followed by centrifugation at 12,000 × g for 5 min to capture the quinolone-bound hydroxyapatite beads. The supernatants were analyzed by HPLC to determine the amount of unbound quinolone. The amount of quinolone bound to the hydroxyapatite beads was calculated by subtracting the amount of unbound quinolone from the total amount of quinolone added to each tube.

Pharmacokinetic experiments and tissue distribution

All animal experiments were conducted according to the guidelines of the Institutional Animal Care and Use Committee of Kanazawa University. Experiments were performed using female ddY mice (8 to 10 weeks old). For the pharmacokinetic study, a dosage of 27.7 μmol/kg of LVFX or LVFX-D$_6$ (equivalent to 10 mg/kg LVFX), or a dosage of 31.3 μmol/kg of NFLX or NFLX-D$_6$ (equivalent to 10 mg/kg NFLX) was injected into the jugular vein of mice. Using heparinized capillary tubes, blood samples were collected from the intraorbital venous plexus of the mice under diethyl ether anesthesia at fixed time intervals. The plasma was separated by

centrifugation and stored at -80°C until assayed. Acetonitrile was added to each plasma sample, and the samples were mixed by vortexing and then centrifuged at 12,000 × g for 10 min. Sample supernatants were analyzed by HPLC. For determining tissue distribution, mice were sacrificed by decapitation at 2 h after a single injection, and multiple tissues, including tibia, bone marrow, brain, heart, lung, liver, spleen, intestine, kidney, and muscle, were dissected. The tibiae were demineralized by incubation in 200 μl of concentrated HCl at 60°C for 2 h; then 400 μl of 10 M NaOH were added, and the samples were mixed at room temperature for 3 h. The solutions were neutralized by adding 200 μl of concentrated HCl and 1 ml of 1 M phosphate buffer (pH 7.0). The other tissues were homogenized in saline, and 200 μl of each homogenate were mixed with 200 μl of 5 M NaOH at room temperature for 3 h. The solutions were neutralized by adding 200 μl of 5 M HCl and 1 ml of 1 M phosphate buffer. This method resulted in the hydrolysis of more than 95% of LVFX-D_6 and NFLX-D_6 to LVFX and NFLX, respectively. To determine the extent of biological hydrolysis of LVFX-D_6 and NFLX-D_6 to LVFX and NFLX-ga, respectively, in the tissues, 1 ml of 1 M phosphate buffer was added to each tissue homogenate without the addition of NaOH and HCl. The digested tissues were extracted twice with chloroform to recover LVFX, NFLX, and NFLX-ga, and the combined chloroform extracts were evaporated. The residues were reconstituted with a HPLC mobile phase; each sample was filtered through a Millex-HV 0.45-μm filter (Millipore, MA, USA), and the flow-through was analyzed by HPLC.

Antibiotic effectiveness in a mouse model of osteomyelitis

Female ddY mice (8 to 10 weeks old) were inoculated with *S. aureus* (JCM 2413, RIKEN, Saitama, Japan) to create experimental osteomyelitis. Briefly, the right tibia was exposed under diethyl ether anesthesia, and a small hole was drilled in the proximal third portion of the tibia with a 26-gauge needle. One microliter of an *S. aureus* suspension containing 10^5 colony-forming units (cfu) was injected into the cavity, and the hole and skin were sealed with medical tissue glue (Aron Alpha A, Sankyo Inc., Tokyo, Japan). On the following day, 110.7 μmol/kg of LVFX or LVFX-D_6 (equivalent to 40 mg/kg LVFX), or 125.3 μmol/kg of

NFLX or NFLX-D$_6$ (equivalent to 40 mg/kg NFLX) were injected via jugular vein. The mice were sacrificed by decapitation at fixed time intervals, and the infected right tibiae were dissected. Soft tissues were removed from the tibiae, and the tibiae were pulverized in 1 ml of saline. The suspensions were serially diluted in saline, and 0.025-ml aliquots of each dilution were plated onto Heart Infusion agar plates (Nissui Pharmaceutical Co. Ltd., Tokyo, Japan). The plates were incubated overnight at 37°C, and the colonies were counted.

Results

Synthesis and antibiotic activity of L-Asp hexapeptide-conjugated quinolones

LVFX was conjugated with L-Asp hexapeptide via a glycolyl ester, and NFLX was conjugated via a glycolyl amide and subsequent succinate ester (Fig. 1). The synthetic yields of LVFX-D$_6$ and NFLX-D$_6$ from starting materials were 18.3 and 10.3%, respectively. The content of impurities such as LVFX in LVFX-D$_6$ and NFLX or NFLX-ga in NFLX-D$_6$ was approximately 0.5% for each preparation, as determined by HPLC analysis. The minimum inhibitory concentrations (MICs) of LVFX, LVFX-D$_6$, NFLX, NFLX-ga, and NFLX-D$_6$ with respect to *S. aureus* were determined by the serial dilution method (Table I). The conjugation of L-Asp hexapeptide significantly decreased the antibiotic activity of LVFX and NFLX; the activities of the non-conjugated forms were approximately 100-fold those of the conjugated forms. The MIC of NFLX-ga, which was expected to be generated through the biological hydrolysis of NFLX-D$_6$, was 50% of the MIC of NFLX.

Binding affinity of L-Asp hexapeptide-conjugated quinolones to hydroxyapatite

At concentrations of 10 nmol/ml and lower, the amounts of LVFX-D$_6$ and NFLX-D$_6$ that bound to hydroxyapatite were 10-fold the amounts of bound LVFX and NFLX, respectively (Fig. 2). However, the difference between the amounts of hydroxyapatite-bound LVFX and LVFX-D$_6$ was less at 30 nmol/ml (2.0 nmol of LVFX versus 3.4 nmol of LVFX-D$_6$ per 100 µg of hydroxyapatite). Appreciable quantities of NFLX and NFLX-ga did not bind to hydroxyapatite until their concentrations reached 30 µM.

Pharmacokinetics and tissue distribution of L-Asp hexapeptide-conjugated quinolones

After a single intravenous injection of LVFX, LVFX-D$_6$, NFLX, or NFLX-D$_6$, the concentrations of the compounds in bone and bone marrow were determined (Fig. 3). The amount of LVFX-D$_6$ in bone was approximately 100-fold that of LVFX at 2 h after injection, and LVFX-D$_6$ was retained in bone at a concentration 100-fold that of LVFX after 7 days.

Furthermore, the hydrolysis of LVFX-D$_6$ maintained LVFX in the bone marrow for at least 7 days, whereas in the group receiving LVFX, LVFX could not be detected in the bone marrow after 1 day. Similarly, the level of NFLX-D$_6$ in bone was approximately 100-fold that of NFLX at 3 days after injection, and substantial amounts of NFLX-D$_6$ were retained in bone for at least 7 days. NFLX was undetectable by day 7. Neither NFLX nor NFLX-ga was detectable in bone marrow after an injection of NFLX or NFLX-D$_6$, respectively.

The plasma-concentration time courses of LVFX, LVFX-D$_6$, NFLX, and NFLX-D$_6$ after a single intravenous injection revealed biphasic behavior of these compounds (Fig. 4). The plasma concentrations of the conjugated quinolones were 2- to 3-fold those of the non-conjugated quinolones initially after injection, whereas the half-life in the plasma was similar between the conjugated and non-conjugated quinolones during the elimination phase. The plasma concentrations of LVFX-D$_6$ and NFLX-D$_6$ were higher than those of LVFX and NFLX, respectively, immediately after injection, but they rapidly decreased, falling to levels similar to those of LVFX and NFLX by 30 min. After an injection of LVFX-D$_6$, LVFX, which might have been generated from LVFX-D$_6$, appeared in the plasma; its concentration slowly decreased, and LVFX was not detectable after 90 min. In contrast, NFLX and NFLX-ga were not detected in the plasma until 6 h after an injection of NFLX-D$_6$.

At 2 h after a single intravenous injection, the apparent plasma-to-tissue concentration ratios (Kp,app) of LVFX, LVFX-D$_6$, NFLX, and NFLX-D$_6$ were determined (Fig. 5). In most of the soft tissues examined, except lung and kidney tissues, LVFX-D$_6$ exhibited a restricted tissue distribution relative to LVFX after the injection of each, and LVFX was not detected in any of the soft tissues after an LVFX-D$_6$ injection. NFLX-D$_6$ also exhibited more limited tissue distribution, except in kidney tissue, than NFLX after their respective injections, and neither NFLX nor NFLX-ga was detected in the soft tissues after NFLX-D$_6$ injection.

Antibiotic effectiveness of L-Asp hexapeptide-conjugated quinolones in a mouse model of osteomyelitis

The antibiotic effectiveness of LVFX, LVFX-D$_6$, NFLX, and NFLX-D$_6$ was evaluated by counting the *S. aureus* colonies remaining in inoculated tibiae after a single intravenous injection of each compound (Fig. 6). In untreated control mice, the cfu of *S. aureus* reached a plateau at 2 days after inoculation. With the injection of either LVFX or LVFX-D$_6$ on the day following *S. aureus* inoculation, a slight reduction in cfu was observed. However, the antibiotic effectiveness of LVFX was temporary; after 6 days, the cfu recovered to levels similar to those in untreated control mice. A prolonged antibiotic effect was observed in mice treated with LVFX-D$_6$, which suppressed the growth of *S. aureus* for at least 6 days. Conversely, neither NFLX nor NFLX-D$_6$ displayed any antibiotic efficacy in the osteomyelitis mouse model (data not shown).

Discussion

In this study we examined the pharmacokinetics and pharmacodynamics of quinolones conjugated with L-Asp hexapeptide as a bone-targeting carrier. We demonstrated that the conjugated quinolones localize to bone, where they were retained for longer times compared with the non-conjugated quinolones and exhibit prolonged antibiotic effects in mice with osteomyelitis.

Quinolones act by inhibiting bacterial topoisomerase II, which is responsible for the replication of double-stranded DNA, and they therefore must cross the bacterial membrane to be effective (26, 27). Specifically, the 3-carboxylate group, a basic structure of quinolones, mediates binding to topoisomerase II (28). As this structure would be obstructed by the direct conjugation of LVFX to the L-Asp hexapeptide moiety, we created a glycolyl ester of LVFX in order to introduce a biologically hydrolysable spacer between LVFX and the L-Asp hexapeptide. To avoid modification of the 3-carboxylate moiety of NFLX, we conjugated L-Asp hexapeptide to the secondary amine of the piperazine ring. However, NFLX-D_6 had substantially reduced antibiotic activity compared with NFLX and NFLX-ga. It is well known that the accumulation of quinolones in Gram-positive bacteria correlates with the hydrophobicity of the molecule, which implies that quinolones cross bacterial membranes by simple diffusion (29-31). The partition coefficients of the conjugated quinolones in n-octanol/aqueous buffer and chloroform/aqueous buffer were approximately 100-fold less than those of the non-conjugated quinolones (data not shown). Thus, the conjugation of hydrophilic amino acids, specifically L-Asp hexapeptide, reduced the hydrophobicity of the quinolones, and the conjugated quinolones could not cross the bacterial membrane until the L-Asp hexapeptide was removed by ester hydrolysis.

Compared with the non-conjugated quinolones, the conjugated quinolones exhibited increased binding affinity to hydroxyapatite *in vitro* and consistently higher bone concentrations *in vivo*. Furthermore, the hydrolyzed product of LVFX-D_6, LVFX, was detected in the plasma and bone marrow after the injection of LVFX-D_6. These findings strongly support using LVFX-D_6 as an osteomyelitis treatment. Indeed, LVFX-D_6 suppressed the growth of *S. aureus*

for at least 6 days in a mouse model of osteomyelitis, thus exhibiting prolonged antibiotic activity. However, the antibiotic effect of LVFX-D$_6$ was not entirely bactericidal, presumably because the concentration of LVFX generated from hydrolyzed LVFX-D$_6$ was insufficient to kill *S. aureus* in bone. NFLX-D$_6$ showed no efficacy in this model of osteomyelitis, nevertheless NFLX-D$_6$ was highly accumulated in bone at approximately 5-fold the concentration of LVFX-D$_6$. The 3-carboxylate and 4-carbonyl groups in quinolone are known to be responsible for potential chelating property with divalent metals such as calcium existing in bone, and these groups remain intact in NFLX-D$_6$, but not in LVFX-D$_6$ (32). It is also known that the extension of the number of acidic amino acid increases the bone accumulating property of acidic oligopeptide *in vivo* (21). Thus, it was hypothesized that the intact 3-carboxylate and 4-carbonyl groups in NFLX-D$_6$ further augmented the affinity of L-Asp hexapeptide to bone. Although the hydrolyzed product of NFLX-D$_6$, NFLX-ga, was not detected in bone marrow after an injection of NFLX-D$_6$, this might be attributable to a lower detection limit of NFLX-ga compared with LVFX. Given the similar decline in the bone concentrations of NFLX-D$_6$ and LVFX-D$_6$, NFLX-ga might be continuously released. Taken together, we expect that the limited effectiveness of NFLX-D$_6$ in this model of osteomyelitis may be due to both NFLX and NFLX-ga have lower antibiotic activity toward *S. aureus* compared with LVFX. The bactericidal effect of quinolones is concentration dependent, with a higher concentration of quinolone producing a more complete killing effect (33, 34). Thus, a high hydrolytic rate of the conjugated quinolones appears to be important for maximal antibiotic effect.

Quinolones extensively penetrate tissues and consequently may cause adverse effects in the cardiovascular system, central nervous system, skin, liver, musculoskeletal system, and kidneys (35-37). The conjugated quinolones showed reduced tissue distribution, probably owing to their increased hydrophilicity. Both LVFX-D$_6$ and NFLX-D$_6$ were distributed to the kidneys at concentrations 2- to 3-fold those of LVFX and NFLX, respectively, at 2 h after injection. However, the levels of the conjugated quinolones returned to those of the non-conjugated quinolones by 4 h (Fig 7). Quinolones are excreted entirely via the kidneys, and the increased

hydrophilicity of the conjugated quinolones may facilitate their accumulation in the kidneys (38, 39). This renal accumulation may also be partly due to the higher plasma concentration, which is a result of the lower tissue distribution, at an early time after injection. In addition, the acidic oligopeptide was eliminated by renal excretion, and the plasma half-life decreased with increasing number of acidic amino acid residues (21). Thus, the L-Asp hexapeptide altered the renal distribution of quinolones, although the influence of L-Asp hexapeptide on the renal pharmacokinetics, including glomerular filtration, tubular secretion, and tubular re-absorption, remains to be solved. The accumulation of conjugated quinolones could increase the risk of adverse events such as azotemia, nephropathy, and interstitial nephritis; meanwhile, the risk of adverse events involving other tissues may be decreased.

When conjugated to an acidic oligopeptide, the common quinolones LVFX and NFLX are model drugs that highlight the clinical feasibility of using a bone-targeting strategy in the treatment of osteomyelitis. To increase the therapeutic effectiveness of this treatment strategy, other compounds with greater initial antibiotic activity could be used, as peptide conjugation is applicable to molecules of all sizes, including enzymes (22, 40-42). Further modifications should also be considered to ensure biological hydrolysis of acidic oligopeptide-conjugated compounds, although the mechanism of hydrolysis remains to be resolved.

References

1. W.G. Cole, R.E. Dalziel, and S. Leitl. Treatment of acute osteomyelitis in childhood. J Bone Joint Surg Br. 64: 218-223 (1982).

2. E.P. Armstrong and D.R. Rush. Treatment of osteomyelitis. Clin Pharm. 2: 213-224 (1983).

3. D.R. Dirschl and L.C. Almekinders. Osteomyelitis. Common causes and treatment recommendations. Drugs. 45: 29-43 (1993).

4. D.P. Lew and F.A. Waldvogel. Osteomyelitis. N Engl J Med. 336: 999-1007 (1997).

5. P.J. Carek, L.M. Dickerson, and J.L. Sack. Diagnosis and management of osteomyelitis. Am Fam Physician. 63: 2413-2420 (2001).

6. J.T. Mader, M. Ortiz, and J.H. Calhoun. Update on the diagnosis and management of osteomyelitis. Clin Podiatr Med Surg. 13: 701-724 (1996).

7. J.T. Mader, D. Mohan, and J. Calhoun. A practical guide to the diagnosis and management of bone and joint infections. Drugs. 54: 253-264 (1997).

8. M.P. Weinstein, C.W. Stratton, H.B. Hawley, A. Ackley, and L.B. Reller. Multicenter collaborative evaluation of a standardized serum bactericidal test as a predictor of therapeutic efficacy in acute and chronic osteomyelitis. Am J Med. 83: 218-222 (1987).

9. K.W. Klemm. Antibiotic bead chains. Clin Orthop Relat Res. 295: 63-76 (1993).

10. D.A. Wininger and R.J. Fass. Antibiotic-impregnated cement and beads for orthopedic infections. Antimicrob Agents Chemother. 40: 2675-2679 (1996).

11. C.G. Ambrose, G.R. Gogola, T.A. Clyburn, A.K. Raymond, A.S. Peng, and A.G. Mikos. Antibiotic microspheres: preliminary testing for potential treatment of osteomyelitis. Clin Orthop Relat Res. 415: 279-285 (2003).

12. C.G. Ambrose, T.A. Clyburn, K. Louden, J. Joseph, J. Wright, P. Gulati, G.R. Gogola, and A.G. Mikos. Effective treatment of osteomyelitis with biodegradable microspheres in a rabbit model. Clin Orthop Relat Res. 421: 293-299 (2004).

13. B. Buranapanitkit, V. Srinilta, N. Ingviga, K. Oungbho, A. Geater, and C. Ovatlarnporn. The efficacy of a hydroxyapatite composite as a biodegradable antibiotic delivery system. Clin

Orthop Relat Res. 424: 244-252 (2004).

14. U. Joosten, A. Joist, G. Gosheger, U. Liljenqvist, B. Brandt, and C. von Eiff. Effectiveness of hydroxyapatite-vancomycin bone cement in the treatment of Staphylococcus aureus induced chronic osteomyelitis. Biomaterials. 26: 5251-5258 (2005).

15. A. Oldberg, A. Franzén, and D. Heinegård. Cloning and sequence analysis of rat bone sialoprotein (osteopontin) cDNA reveals an Arg-Gly-Asp cell-binding sequence. Proc Natl Acad Sci U S A. 83: 8819-8823 (1986).

16. A. Oldberg, A. Franzén, and D. Heinegård. The primary structure of a cell-binding bone sialoprotein. J Biol Chem. 263: 19430-19432 (1988).

17. W.T. Butler. The nature and significance of osteopontin. Connect Tissue Res. 23: 123-136 (1989).

18. T. Nagata, C.G. Bellows, S. Kasugai, W.T. Butler, and J. Sodek. Biosynthesis of bone proteins [SPP-1 (secreted phosphoprotein-1, osteopontin), BSP (bone sialoprotein) and SPARC (osteonectin)] in association with mineralized-tissue formation by fetal-rat calvarial cells in culture. Biochem J. 274: 513-520 (1991).

19. S. Kasugai, R. Todescan Jr., T. Nagata, K.L. Yao, W.T. Butler, and J. Sodek. Expression of bone matrix proteins associated with mineralized tissue formation by adult rat bone marrow cells in vitro: inductive effects of dexamethasone on the osteoblastic phenotype. J Cell Physiol. 147: 111-120 (1991).

20. S. Kasugai, T. Nagata, and J. Sodek. Temporal studies on the tissue compartmentalization of bone sialoprotein (BSP), osteopontin (OPN), and SPARC protein during bone formation in vitro. J Cell Physiol. 152: 467-477 (1992).

21. T. Sekido, N. Sakura, Y. Higashi, K. Miya, Y. Nitta, M. Nomura, H. Sawanishi, K. Morito, Y. Masamune, S. Kasugai, K. Yokogawa, and K. Miyamoto. Novel drug delivery system to bone using acidic oligopeptide: pharmacokinetic characteristics and pharmacological potential. J Drug Target. 9: 111-121 (2001).

22. S. Kasugai, R. Fujisawa, Y. Waki, K. Miyamoto, and K Ohya. Selective drug delivery system

to bone: small peptide (Asp)6 conjugation. J Bone Miner Res. 15: 936-943 (2000).

23. I. Phillips, A. King, and K. Shannon. In vitro properties of the quinolones. In V.T. Andriole (ed.), The quinolones, Academic Press, New York, 1988, pp. 83-117.

24. J.T. Mader. Fluoroquinolones in bone and joint infections. In W.E. Sanders Jr. and C.C. Sanders (eds.), Fluoroquinolones in the treatment of infectious diseases, Physicians & Scientists, Illinois, 1990, pp. 71-86.

25. J.T. Mader, J.S. Cantrell, and J. Calhoun. Oral ciprofloxacin compared with standard parenteral antibiotic therapy for chronic osteomyelitis in adults. J Bone Joint Surg Am. 72: 104-110 (1990).

26. R.J. Lewis, F.T. Tsai, and D.B. Wigley. Molecular mechanisms of drug inhibition of DNA gyrase. Bioessays. 18: 661-671 (1996).

27. L.L. Shen and D.T.W. Chu. Type II DNA topoisomerases as antibacterial targets. Curr Pharm Des. 2: 195-208 (1996).

28. T.D. Gootz and K.E. Brighty. Fluoroquinolone antibacterials: SAR mechanism of action, resistance, and clinical aspects. Med Res Rev. 16: 433-486 (1996).

29. Y. Hirakata, M. Kaku, R. Mizukane, K. Ishida, N. Furuya, T. Matsumoto, K. Tateda, and K. Yamaguchi. Potential effects of erythromycin on host defense systems and virulence of Pseudomonas aeruginosa. Antimicrob Agents Chemother. 36: 1922-1927 (1992).

30. S. Bazile, N. Moreau, D. Bouzard, and M. Essiz. Relationships among antibacterial activity, inhibition of DNA gyrase, and intracellular accumulation of 11 fluoroquinolones. Antimicrob Agents Chemother. 36: 2622-2627 (1992).

31. L.J. Piddock, Y.F. Jin, and D.J. Griggs. Effect of hydrophobicity and molecular mass on the accumulation of fluoroquinolones by Staphylococcus aureus. J Antimicrob Chemother. 47: 261-270 (2001).

32. J.M. Domagala. Structure-activity and structure-side-effect relationships for the quinolone antibacterials. J Antimicrob Chemother. 33: 685-706 (1994).

33. J. Blaser, B.B. Stone, M.C. Groner, and S.H. Zinner. Comparative study with enoxacin and

netilmicin in a pharmacodynamic model to determine importance of ratio of antibiotic peak concentration to MIC for bactericidal activity and emergence of resistance. Antimicrob Agents Chemother. 31: 1054-1060 (1987).

34. S.L. Preston, G.L. Drusano, A.L. Berman, C.L. Fowler, A.T. Chow, B. Dornseif, V. Reichl, J. Natarajan, and M. Corrado. Pharmacodynamics of levofloxacin: a new paradigm for early clinical trials. JAMA. 279: 125-129 (1998).

35. J.M. Blondeau. Expanded activity and utility of the new fluoroquinolones: a review. Clin Ther. 21: 3-40 (1999).

36. J.J. Schentag and B.E. Scully. Antibacterial agents-quinolones. In V.L. Yu and T.C. Merigan Jr. (eds.), Antimicrobial therapy and vaccines, Williams & Wilkins, Baltimore, 1999, pp. 875-901.

37. J.A. O'Donnell and S.P. Gelone. Fluoroquinolones. Infect Dis Clin North Am. 14: 489-513 (2000).

38. R. Davis and H.M. Bryson. Levofloxacin. A review of its antibacterial activity, pharmacokinetics and therapeutic efficacy. Drugs. 47: 677-700 (1994).

39. P. Ball. The quinolones, history and overview. In V.T. Andriole (ed.), The quinolones, Academic Press, New York, 1998, pp. 1-28.

40. K. Yokogawa, K. Miya, T. Sekido, Y. Higashi, M. Nomura, R. Fujisawa, K. Morito, Y. Masamune, Y. Waki, S. Kasugai, and K Miyamoto. Selective delivery of estradiol to bone by aspartic acid oligopeptide and its effects on ovariectomized mice. Endocrinology. 142: 1228-1233 (2001).

41. T. Nishioka, S. Tomatsu, M.A. Gutierrez, K. Miyamoto, G.G. Trandafirescu, P.L. Lopez, J.H. Grubb, R. Kanai, H. Kobayashi, S. Yamaguchi, G.S. Gottesman, R. Cahill, A. Noguchi, and W.S. Sly. Enhancement of drug delivery to bone: characterization of human tissue-nonspecific alkaline phosphatase tagged with an acidic oligopeptide. Mol Genet Metab. 88: 244-255 (2006).

42. J.L. Millán, S. Narisawa, I. Lemire, T.P. Loisel, G. Boileau, P. Leonard, S. Gramatikova, R. Terkeltaub, N. Pleshko Camacho, M.D. McKee, P. Crine, and M.P. Whyte. Enzyme replacement

therapy for murine hypophosphatasia. J Bone Miner Res. in press (2007).

Figure legends

Fig. 1. Molecular structures of LVFX, glycolyl ester of LVFX (LVFX-ga), LVFX-D_6, NFLX, glycolyl-NFLX (NFLX-ga), glycolyl-NFLX hemisuccinate (NFLX-ga-suc), and NFLX-D_6.

Fig. 2. Concentration-dependent binding curves of L-Asp hexapeptide-conjugated and non-conjugated quinolones to hydroxyapatite. Final concentrations of 0.1 to 30 μM of each compound, A) LVFX (○) and LVFX-D_6 (●), and B) NFLX (○), NFLX-ga (△), and NFLX-D_6 (●), were incubated with 100 μg of hydroxyapatite at 37°C for 1 h. The unbound quinolone was separated from the bound quinolone by centrifugation and the concentration of unbound quinolone in the supernatant was measured. The amount of bound quinolone was calculated by subtracting the unbound from the total. L-Asp hexapeptide conjugation significantly increased the binding affinity of quinolones to hydroxyapatite. Each point with a bar represents the mean ± SE of 3-6 experiments.

Fig. 3. Time course of bone and bone marrow concentrations of L-Asp hexapeptide-conjugated and non-conjugated quinolones. A dosage of A) 27.7 μmol/kg of LVFX (○) or LVFX-D_6 (●), or B) 31.3 μmol/kg of NFLX (○) or NFLX-D_6 (●) was intravenously injected into mice, and the concentrations in the tibia were determined at the indicated time points. The L-Asp hexapeptide-conjugated quinolones were concentrated and retained in bone at approximately 100-fold the concentrations of non-conjugated quinolones for at least 7 days after injection. C) In bone marrow, LVFX was detected at 2 h after an injection of LVFX (○) or LVFX-D_6 (●). The LVFX concentration declined to an undetectable level within 1 day after LVFX injection, whereas LVFX continued to be generated for at least 7 days after LVFX-D_6 injection. Neither NFLX nor NFLX-ga was detected in bone marrow after injection of either NFLX or NFLX-D_6, respectively. Each point with a bar represents the mean ± SE of four mice.

Fig. 4. Time course of plasma concentrations of L-Asp hexapeptide-conjugated and

non-conjugated quinolones. A dosage of A) 27.7 μmol/kg of LVFX (○) or LVFX-D$_6$ (●), or B) 31.3 μmol/kg of NFLX (○) or NFLX-D$_6$ (●) was intravenously injected into mice, and the concentrations in plasma were determined at the indicated time points. All the compounds were eliminated from the plasma in a biphasic manner. The plasma concentrations of the conjugated quinolones were 2- to 3-fold those of the non-conjugated quinolones initially after injection. However, the half-life was similar between the conjugated and non-conjugated quinolones during the elimination phase. The hydrolyzed product LVFX (■), which was shown in A), was detected in the plasma after LVFX-D$_6$ injection, and LVFX was eliminated slowly from the plasma. The predicted hydrolyzed products of NFLX-D$_6$ (NFLX and NFLX-ga) were not detected in the plasma after NFLX-D$_6$ injection. Each point with a bar represents the mean ± SE of four mice.

Fig. 5. Tissue distribution of L-Asp hexapeptide-conjugated and non-conjugated quinolones. A dosage of A) 27.7 μmol/kg of LVFX (□) or LVFX-D$_6$ (■), or B) 31.3 μmol/kg of NFLX (□) or NFLX-D$_6$ (■) was intravenously injected into mice, and the concentration of each compound was determined in the indicated tissues at 2 h after injection. The amounts of the L-Asp hexapeptide-conjugated quinolones were less than the amounts of the non-conjugated quinolones in most tissues, with the exception of lung and kidney tissues. The predicted products of hydrolysis (LVFX, NFLX, and NFLX-ga) were not detected in any of the soft tissues examined. Each column with a bar represents the mean ± SE of four mice. Kp,app; apparent plasma-to-tissue concentration ratios.

Fig. 6. Antibiotic effectiveness of LVFX and LVFX-D$_6$ in a mouse model of osteomyelitis. One microliter containing 10^5 cfu of *S. aureus* was inoculated into the tibiae of mice. The following day, LVFX (○) or LVFX-D$_6$ (●) at 110.7 μmol/kg was intravenously injected, and the quantity of surviving *S. aureus* colonies was determined at the indicated time points. The cfu in untreated control mice (△) reached a plateau 2 days post-inoculation, whereas both LVFX and LVFX-D$_6$ significantly suppressed the growth of *S. aureus*. The antibiotic efficacy of LVFX-D$_6$ continued

for at least 6 days after injection, but the effectiveness of LVFX was temporary. Each point with a bar represents the mean ± SE of 8-12 mice. *, **; significantly different from untreated control mice at $p < 0.05$ and $p < 0.01$, respectively. [†]; significantly different from LVFX-treated mice at $p < 0.01$.
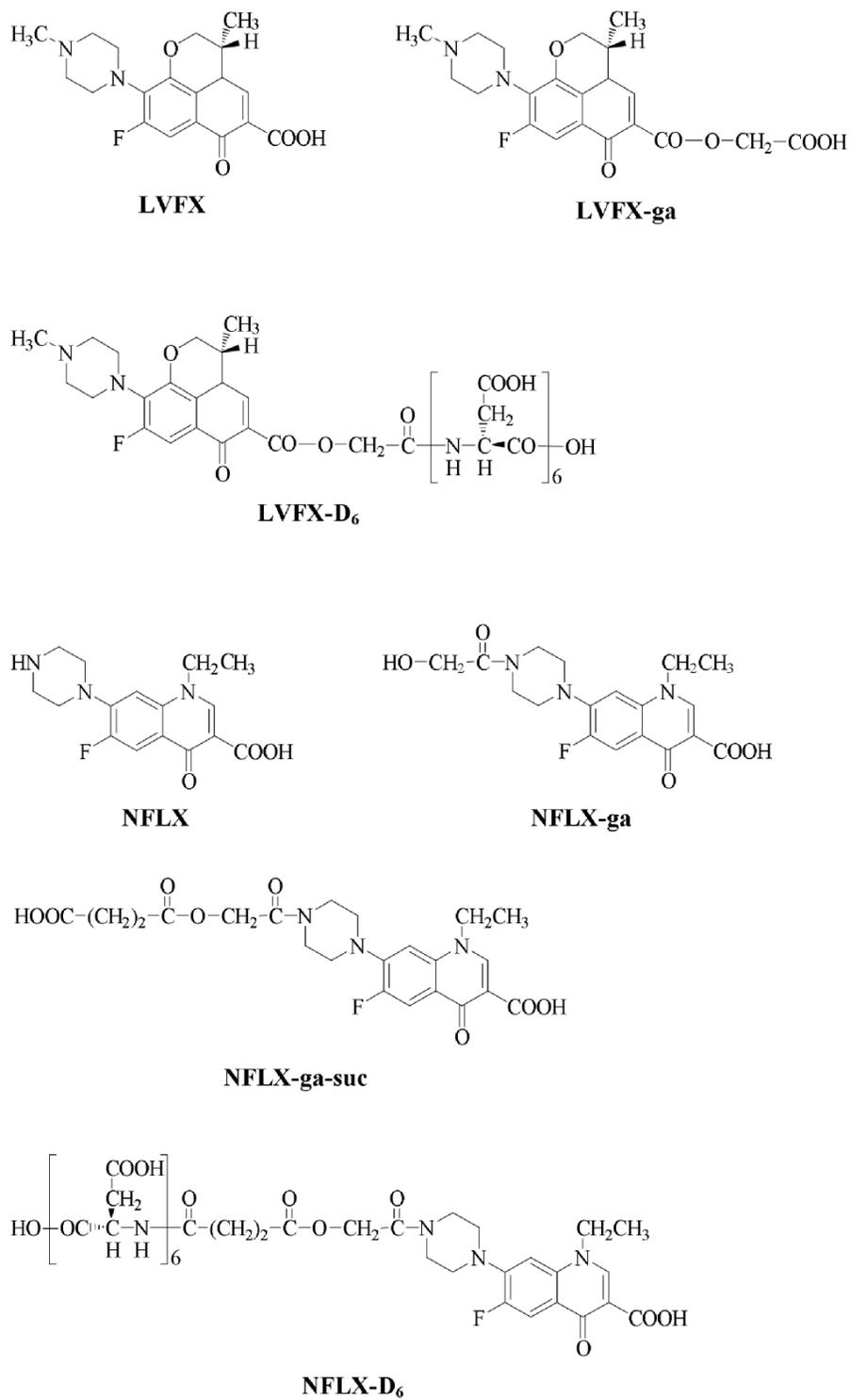
Fig. 7. Time course of kidney concentrations of L-Asp hexapeptide-conjugated and non-conjugated quinolones. A dosage of A) 27.7 μmol/kg of LVFX (○) or LVFX-D$_6$ (●), or B) 31.3 μmol/kg of NFLX (○) or NFLX-D$_6$ (●) was intravenously injected into mice, and the concentrations in kidney were determined at the indicated time points. The L-Asp hexapeptide-conjugated quinolones were concentrated in kidney at approximately two-fold the concentrations of non-conjugated quinolones at 2 h after injection. At 4 h, however, the kidney concentrations of the L-Asp hexapeptide-conjugated quinolones fell in the similar level as non-conjugated quinolones. Each point with a bar represents the mean ± SE of four mice.

Table I. *In vitro* antibiotic activities of L-Asp hexapeptide-conjugated and non-conjugated quinolones against *Staphylococcus aureus*.
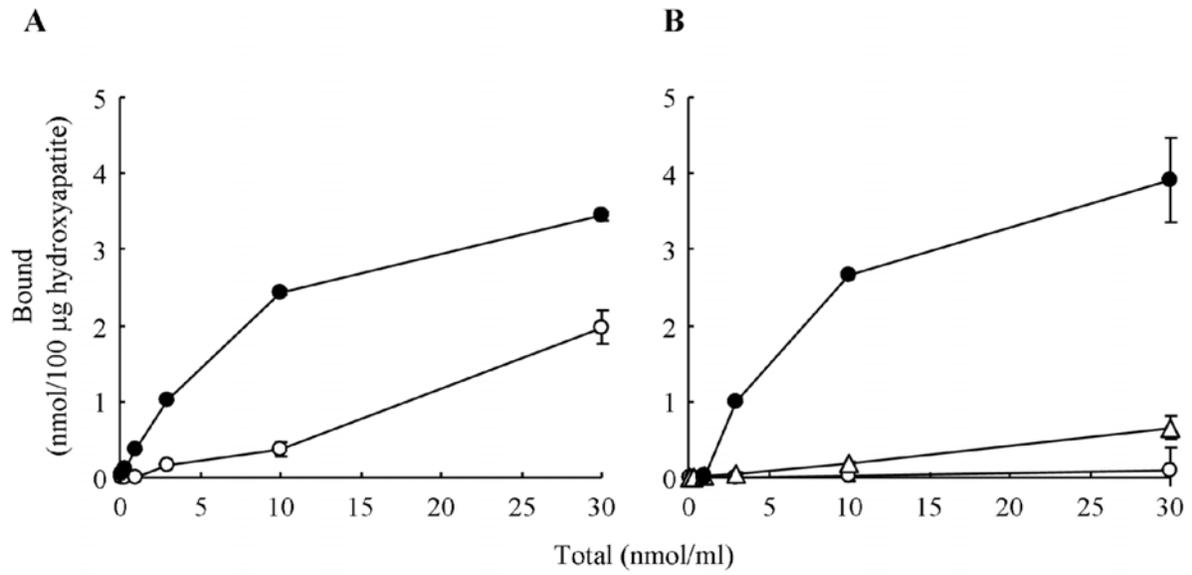
Compound	MIC[a] (nmol/ml)
LVFX	0.35
LVFX-D$_6$	44.3
NFLX	3.13
NFLX-ga	6.26
NFLX-D$_6$	200

[a]MIC, minimum inhibitory concentration; the lowest concentration of a compound that inhibited visible growth of *S. aureus* after overnight incubation at 37°C in Mueller-Hinton broth.
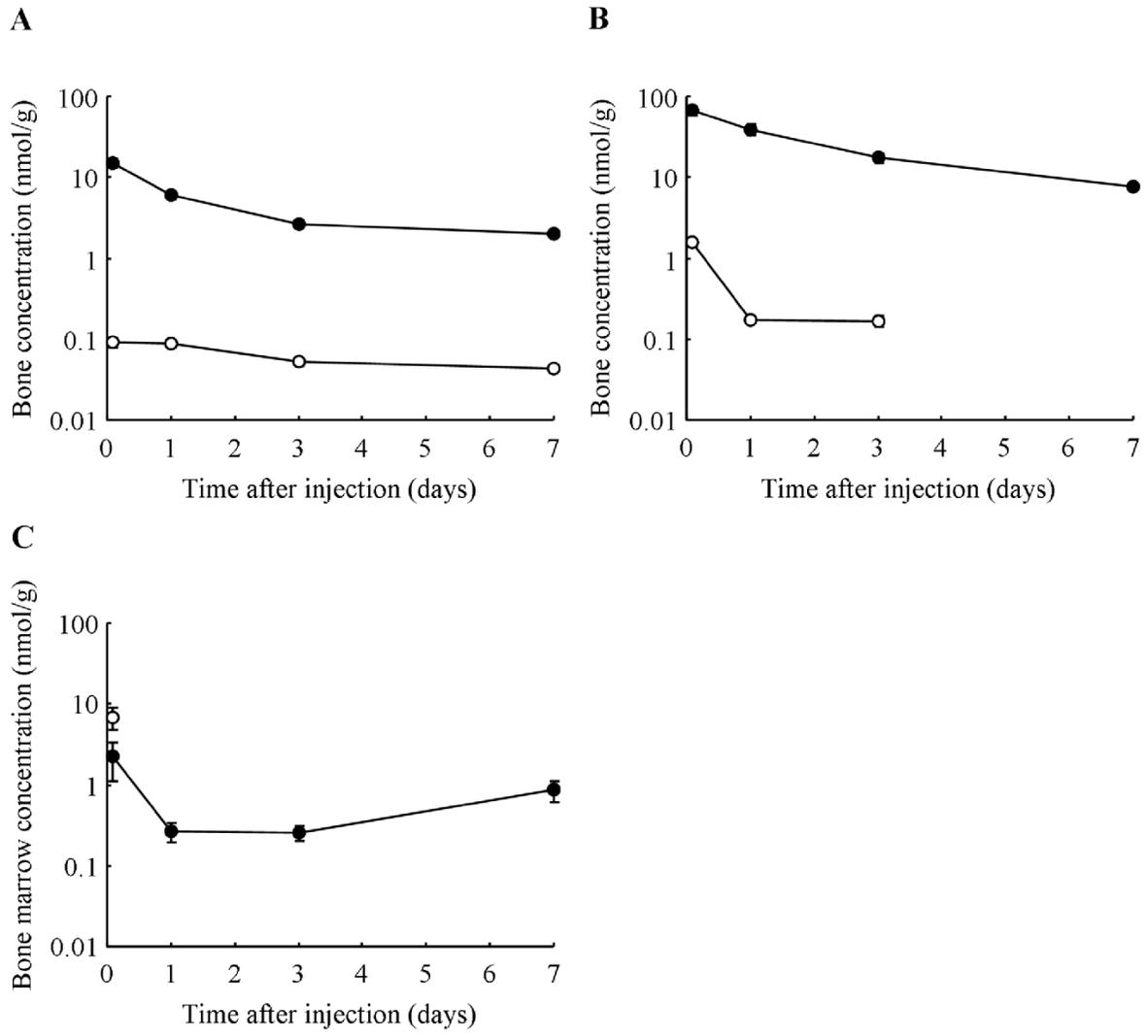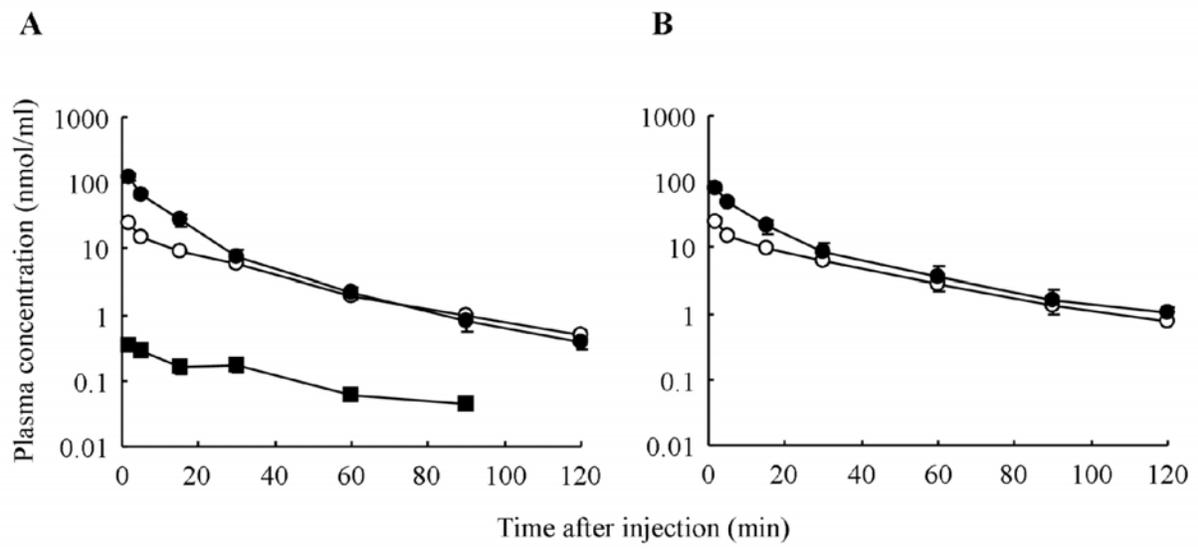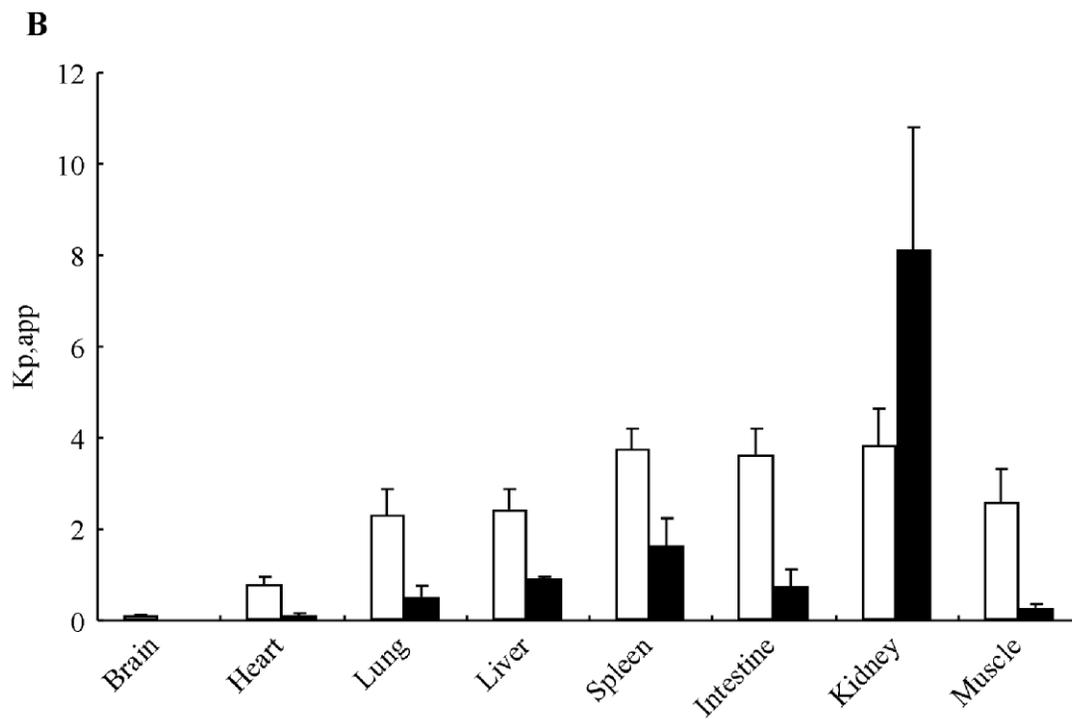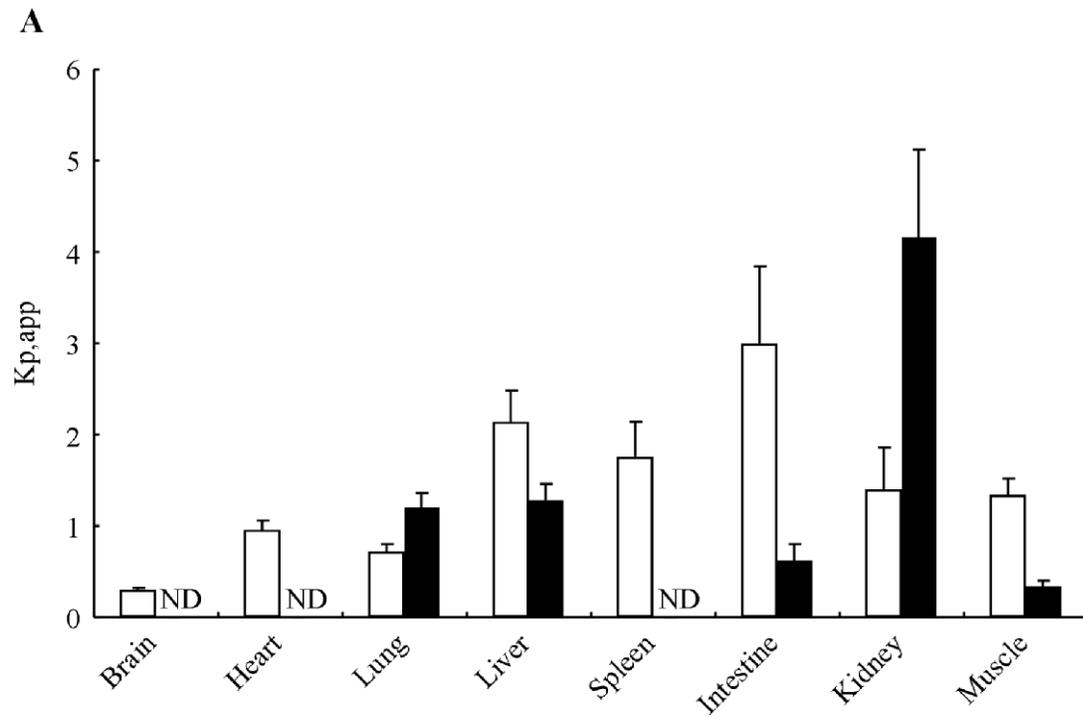
Fig. 1

LVFX

LVFX-ga

LVFX-D$_6$

NFLX

NFLX-ga

NFLX-ga-suc

NFLX-D$_6$

Fig. 2

Fig. 3

A

B

C

Fig. 4

A

B

Plasma concentration (nmol/ml)

Time after injection (min)

Fig. 5

A

B

Fig. 6

Fig. 7